Aerosol and Air Quality Research, 13: 209–218, 2013

ISSN: 1680-8584 print / 2071-1409 online
doi: 10.4209/aaqr.2012.02.0037

Influence of CO and H_2 Concentrations on Coal Gas Dechlorination by Supported Manganese Oxide Sorbent

Ting Ke Tseng, Ling Wang, Hsin Chu*

Department of Environmental Engineering and Research Center for Energy Technology and Strategy, National Cheng Kung University, 1 University Road, Tainan 701, Taiwan

ABSTRACT

The Mn_2O_3/SiO_2 sorbent prepared by incipient wetness impregnation was investigated for the elimination of chlorine species produced from coal gasification. The experiments were conducted in a fixed-bed reactor at 673 K with the Mn_2O_3/SiO_2 sorbent at various CO and H_2 concentrations to evaluate their influences on the dechlorination performance. It was observed that the absence of inlet H_2 led to a drastic decrease in the sorbent capacity; i.e., the presence of H_2 was essential for achieving dechlorination. Furthermore, the concentration of CO seemed to have no obvious effect on the HCl removal.

Through the breakthrough experiments, X-ray powder diffractometer, and Fourier transform infrared spectroscopy analysis, the overall dechlorination mechanism of the Mn_2O_3/SiO_2 sorbent in a chlorine-containing coal gas system was successfully described in this study. The mechanism consisted of three major routes: (a) Mn_2O_3 reacted with HCl to form $MnCl_2$, (b) Mn_2O_3 was first reduced into Mn_3O_4 and then reacted with HCl to produce $MnCl_2$, and (c) without the involvement of HCl in the dechlorination experiments, the Mn_2O_3 contained in the fresh sorbent was first reduced to Mn_3O_4 and then to MnO under the strong reducing atmosphere provided by CO and/or H_2.

Keywords: Dechlorination; Sorbent; Mn_2O_3; H_2; IGCC.

INTRODUCTION

Since the Industrial Age, the balance between energy supply and environmental protection has been confronted with enormous challenges. Therefore, with its abundance and relatively low and constant price, coal is a popular candidate to manage continuous growth of global energy demand. In the coming decades technology of clean energy production from coal becomes critical.

Integrated gasification combined cycle (IGCC), as an advanced coal technology, has recently provided the world incentive to move toward a cleaner and more efficient energy use. However, since IGCC generates electricity through coal gasification, impurities such as sulfur and chlorine contained in coal will be released in the form of H_2S and HCl, respectively, during the process of gasification (Yang *et al.*, 2006; Lin *et al.*, 2010; Tu *et al.*, 2011). To achieve the goal of a low pollution to the environment, IGCC requires treatments for these deleterious emissions prior to the combustion of coal gas for electricity production.

Considering absorption by sorbents at high temperature as a most frequent, relatively direct and convenient way to remove contaminants from coal gas, options for desulfurization and dechlorination are various. Popular choices for H_2S removal include the Ca- (Li *et al.*, 2007), Fe- (Ko *et al.*, 2006), Mn- (Bakker *et al.*, 2003; Ko *et al.*, 2005), Zn-based sorbent (Bu *et al.*, 2008), and mixed metal oxide sorbent (Ko *et al.*, 2007; Lou *et al.*, 2009; Chang *et al.*, 2012); those for HCl removal include the Ca- (Yan *et al.*, 2003; Chin *et al.*, 2005), Na-based sorbent (Nunokawa *et al.*, 2008), and industrial catalyst mixed with multiple components (Dou *et al.*, 2005). Due to the fact that a high percentage of the pollution emitted by coal gasification comes from sulfides, research activities focusing on desulfurization have been widely studied; while relatively little attention has been paid to dechlorination.

Nevertheless, HCl was found to be able to exert a negative influence on the capacity of sulfur removal (Kiil *et al.*, 2002); thereby, taking the possibility of simultaneous sulfur removal into consideration, sorbents capable of eliminating both species will be a better option. Previous literatures have reported on sorbent based upon manganese having promising desulfurization potential (Westmoreland and Harrison, 1976; Atimtay, 2001). Laboratory scale experiments were also conducted showing that Mn-based sorbents had high desulfurization performance (Bakker *et al.*, 2003; Ko *et al.*,

* Corresponding author. Tel.: (886)-6-208-0108
Fax: (886)-6-275-2790
E-mail address: chuhsin@mail.ncku.edu.tw

2005). On the basis of potentially removing both species, the Mn-based sorbent emerged as the leading candidate for HCl elimination through thermodynamic screening conducted by the calculation of equilibrium constant. Bakker *et al.* (2003) studied the desulfurization in a fixed-bed reactor at 400 to 1000°C for hot gas cleaning using Mn-based sorbents. The Mn-based sorbents, prepared by wet impregnation consisting of crystalline $MnAl_2O_4$, a small amount of disperse MnO, and an amorphous Mn—Al—O phase, showed high capacity for desulfurization. Furthermore, MnO and $MnAl_2O_4$ were also proved to be feasible for HCl removal.

In this study the main focus was directed toward the co-existing gases since the performance of contaminant removal will be affected by the presence of CO and H_2 (Ko *et al.*, 2006; Tseng *et al.*, 2008). The fact that the extent of influence of these species in coal gas on the performance of HCl removal has not been known completely may suggest the need for further study. This study aims to evaluate the effects of CO and H_2 concentrations on the dechlorination experiments, as well as to carry out a further investigation into the dechlorination mechanism of the Mn_2O_3/SiO_2 sorbent.

METHODS

Material

The Mn_2O_3/SiO_2 sorbent prepared by incipient wetness impregnation on supported materials at room temperature were employed in this research. The supported materials were pure commercial SiO_2 spherical particles (Alfa Aesar, stock #44740), which were crushed and sieved to 30–50 mesh and dried in an oven at 393 K for 12 hours to remove the impurities and remaining water before impregnation. The impregnation was proceeded by spraying an aqueous manganese nitrate solution ($Mn(NO_3)_2{\cdot}4H_2O$) added with appropriate amounts of de-ionized water evenly on SiO_2. Followed by 24 hours of dryness in an oven at 393 K, the impregnated materials were kept at room temperature for 12 hours. Finally, the materials were calcined in airflow conditions at 973 K for 8 hours in a fixed-bed quartz reactor. Sorbents were dried in an oven for 2 hours every time before experiments to remove the remaining water vapor, and every experiment was supplied with 1.0 g sorbent (1.0 cm thick). It should be noted that the nominal weight loading of manganese oxide on SiO_2 was initially 20 wt%, and corrected to approximately 23 wt% through Inductivity coupled plasma-mass spectrometer (ICP-MS) analysis.

Equipment

The experimental apparatus was composed of: (a) a simulated coal gas system, (b) a high-temperature reaction system, and (c) a gas analyzing system.

In the simulated coal gas system, HCl, CO, H_2, and N_2 were supplied from gas cylinders, mixed in a mixer to ensure the gas mixtures were turbulent, and then introduced to the reaction system. The flow rate of HCl were monitored through a mass flow meter (Protec, PC-540), and that of the rest were monitored by IR soap bubble meters (Gilian, Gilibrator-2).

The reaction system consisted of a bench-scale fixed-bed reactor (a 1.5 cm i.d., 1.8 cm o.d., and 85 cm long quartz tube), an electrical furnace, a temperature controller (TTE, TM-4800), and a K-type thermocouple (0.35 cm o.d., 60 cm long). The quartz tube was housed in the electrical furnace, and set with a 200 mesh frit quartz disk 45 cm below the top of the tube to support the sorbents. The K-type thermocouple was inserted into the quartz tube with its tip set above the position of the sorbent for accurate temperature measurement through temperature controller. The frit quartz disk was well paved with a layer of glass wool between sorbents and itself prior to every experiment to avoid unstable pressure and the leakage of the sorbent.

The gas analyzing system contained a HCl analyzer and a Fourier transform infrared spectroscopy (FTIR). The outlet HCl concentration was recorded every twelve minute as the experiments proceeded by an on-line gas filter correlation HCl analyzer (Thermo Electron Corporation, MODEL 15C). It is noteworthy that in the experiments with 0 vol% H_2, the HCl concentration was recorded every two minute rather than twelve due to the sudden breakthrough of the HCl concentration. The FTIR spectrum of the outlet gases from the reactor were obtained on a Perkin Elmer Spectrum One B spectrometer by recording the amount of absorbed light as a function of the scanning wavenumber (cm^{-1}). The recorded IR spectra were processed at a resolution of 4 cm^{-1} with the use of Time Base 2.0 software.

Conditions

The actual composition of coal gas produced by coal gasification varies over a wide range, depending on the type of coal, the gasification temperature, and the model of gasifier (Wakker *et al.*, 1993; Krishnan *et al.*, 1994). The dechlorination experiments were carried out in a simulated coal gas system containing 3,000 ppm HCl, 25 vol% CO, 15 vol% H_2, and N_2 as a balance gas. Hence, in this study various concentrations of CO and H_2 were applied to the fixed-bed reactor to evaluate their effects on the dechlorination performance. The inlet concentrations of CO included 0, 10, 25 vol%, and that of H_2 included 0, 10, and 15 vol%. The experiments with 500, 1,000, and 3,000 ppm HCl were carried out in advance and the best sorbent capacity was achieved when the inlet HCl concentration was 3,000 ppm. Hence in this research the reaction system was fed with 3,000 ppm HCl.

The influence of temperature on the reaction was studied at 573–873 K, and the optimum operating temperature for HCl removal was found at 673 K. Accordingly, in this research the dechlorination experiments were all carried out at 673 K ensuring the best possible outcome. Moreover, the weight hourly space velocity (WHSV) was all set at 6,000 mL/h/g. The nominal compositions of these gas mixtures are shown Table 1.

Characterization

The chlorinated sorbents were characterized after the experiments. The crystalline structures of fresh and chlorinated samples were analyzed by a Rigaku D/Max III-V X-ray powder diffractometer (XRD) employing Cu Kα

Table 1. The gas composition of simulated coal gas mixtures.

Reaction Type	HCl Conc. (ppm)	H_2 Conc. (%)	CO Conc. (%)	weight hourly space velocity (mL/h/g)	Temperature (K)
Influence of CO and H_2 concentrations on the dechlorination	3,000	0	0 10 25	6,000	673
		10	0 10 25		
		15	0 10 25		
FTIR spectroscopy for HCl removal	3,000	0	0 10	6,000	673
		10	0 10		

radiation (λ = 1.54056 Å). The applied current and voltage were 30 mA and 20 kV, respectively, and the scan rate was 3°/min. The diffraction patterns were recorded and analyzed using MDI Jade 5.0 software and Powder Diffraction File (PDF) database published by International Centre for Diffraction Data (ICDD).

RESULTS AND DISCUSSION

Influence of CO and H_2 Concentrations on the Dechlorination

To measure the dechlorination capacity, performance of the Mn_2O_3/SiO_2 sorbent can be expressed as sorbent utilization (SU):

$$\text{SU}\ (\%) = \frac{\int_0^t (C_{\text{in}} - C_{\text{out}})\mathrm{d}t}{C_{\text{in}} \times t^*} \times 100\% \quad (1)$$

where C_{in} and C_{out} are the inlet and outlet concentrations of HCl (ppm), respectively; t is the experimental breakthrough time (min), and t^* is the theoretical breakthrough time (min) of the dechlorination process. According to Taiwan Stationary Pollution Source Air Pollutant Emissions Standards, the HCl emissions are regulated within 80 ppm, in which case the experimental breakthrough time was defined as the time from the beginning of the experiment to the point when the outlet HCl concentration reached 80 ppm. As for the theoretical breakthrough time (min), its definition is given as below:

$$t^* = \frac{\left(\frac{WX}{M}\right)A}{F} \quad (2)$$

where W is the weight of the Mn_2O_3/SiO_2 sorbent placed in the reactor (g), X is the actual weight loading of manganese oxide supported on SiO_2 (g/g), M is the molecular weight of the manganese oxide (g/mol), A is the moles of HCl that can be absorbed by one mole of manganese oxide (mol/mol), and F is the molar flow rate of the inlet HCl (mol/min).

A number of chemical reactions were expected to take place in the system when Mn_2O_3/SiO_2 made contact with HCl and other components containing in the simulated syngas. The possible reactions were examined by a thermodynamic point of view.

Standard thermodynamic values obtained for later calculations are listed in Table 2. Table 2 summarize the thermodynamic results for reactions of sorbent with HCl, CO, and H_2, respectively and simultaneously, at various temperatures (400, 500, 600, 800, 1000, and 1500 K). Every positive Gibbs free energy and the related equilibrium constant were highlighted in bold.

Reactions of Mn_2O_3 with CO and H_2 in Table 2 indicate the possibility of the reduction of Mn_2O_3 contained in sorbent to form Mn_3O_4 accompanied by possible production of CO_2 and H_2O. Mn_2O_3 can react with CO to form Mn_3O_4 and CO_2, or with H_2 to form Mn_3O_4 and H_2O. Reaction (3) shows that Mn_2O_3 can react with both CO and H_2 to form Mn_3O_4, CO_2, and H_2O.

The reactions of Mn_2O_3 with HCl accompanied by CO and H_2 to produce $MnCl_2$, CO_2 and H_2O. Mn_2O_3 can react with HCl and CO to form $MnCl_2$, CO_2 and H_2O, or with HCl and H_2 to form $MnCl_2$ and H_2O. Reaction (4) reveals that Mn_2O_3 can react with HCl and both CO and H_2 to produce $MnCl_2$, CO_2, and H_2O.

Reactions (3) has a tendency to form Mn_3O_4 when reacting with CO or/and H_2 due to the strong reducing atmosphere. In addition, the Mn_3O_4 formed from the reduction reaction can subsequently be attacked by the presence of HCl. Same as Reactions (4), Mn_3O_4 can react with HCl and CO to form $MnCl_2$, CO_2, and H_2O, or with HCl and H_2 to form $MnCl_2$ and H_2O. Also, the production of $MnCl_2$, CO_2 and H_2O can be resulted from reaction of Mn_3O_4 with HCl and both CO and H_2. To be noticed, Reaction (5) has the highest equilibrium constant among all of the reaction presented in this study.

Calculated through the following dechlorination reactions (Reactions (3)–(5)), 1 mol of Mn_2O_3 is able to remove 4 mols of HCl.

Table 2. Summary of the thermodynamic calculations for reaction of Mn_2O_3 with CO and H_2

No.	Reaction	Temperature (K)	ΔG (kJ/mol)	K[a]
(3)	$Mn_2O_{3(s)} + \frac{1}{6}CO_{(g)} + \frac{1}{6}H_{2(g)} \rightarrow \frac{2}{3}Mn_3O_{4(s)} + \frac{1}{6}CO_{2(g)} + \frac{1}{6}H_2O_{(g)}$	400	–337.7	1.3E+44
		500	–343.7	8.0E+35
		600	–350.6	3.3E+30
		800	–366.7	8.8E+23
		1000	–384.8	1.3E+20
		1500	–431.2	1.0E+15
(4)	$Mn_2O_{3(s)} + 4HCl_{(g)} + \frac{1}{2}CO_{(g)} + \frac{1}{2}H_{2(g)} \rightarrow 2MnCl_{2(s)} + \frac{1}{2}CO_{2(g)} + \frac{5}{2}H_2O_{(g)}$	400	–597.4	1.0E+78
		500	–558.7	2.3E+58
		600	–520.9	2.2E+45
		800	–447.6	1.7E+29
		1000	–376.3	4.5E+19
		1500	–199.1	8.6E+06
(5)	$Mn_3O_{4(s)} + 6HCl_{(g)} + \frac{1}{2}CO_{(g)} + \frac{1}{2}H_{2(g)} \rightarrow 3MnCl_{2(s)} + \frac{1}{2}CO_{2(g)} + \frac{7}{2}H_2O_{(g)}$	400	–727.3	9.5E+94
		500	–666.2	4.0E+69
		600	–606.1	5.8E+52
		800	–488.0	7.4E+31
		1000	–372.0	2.7E+19
		1500	–83.1	7.8E+02

[a]: equilibrium constant.

$$Mn_2O_{3(s)} + \frac{1}{6}CO_{(g)} + \frac{1}{6}H_{2(g)} \rightarrow \frac{2}{3}Mn_3O_{4(s)} + \frac{1}{6}CO_{2(g)} + \frac{1}{6}H_2O_{(g)} \quad (3)$$

$$Mn_2O_{3(s)} + 4HCl_{(g)} + \frac{1}{2}CO_{(g)} + \frac{1}{2}H_{2(g)} \rightarrow 2MnCl_{2(s)} + \frac{1}{2}CO_{2(g)} + \frac{5}{2}H_2O_{(g)} \quad (4)$$

$$Mn_3O_{4(s)} + 6HCl_{(g)} + \frac{1}{2}CO_{(g)} + \frac{1}{2}H_{2(g)} \rightarrow 3MnCl_{2(s)} + \frac{1}{2}CO_{2(g)} + \frac{7}{2}H_2O_{(g)} \quad (5)$$

Research centered on the effects of CO and H_2 on the performance of HCl elimination was carried out by introducing various amounts of CO and H_2 into the absorption system. The breakthrough curves in Fig. 1 are presented as a plot of dimensionless time t/t^* (min/min) versus HCl concentration (ppm). Every set of the experiments were conducted over three times, thus the error bars in the following figures can ensure the accuracy of the experimental data.

In Fig. 1(a), the Mn_2O_3/SiO_2 sorbent was reacted at 673 K with 3,000 ppm HCl in the presence of 15 vol% H_2 at various CO concentrations. The breakthrough dimensionless time at 0, 10, and 25 vol% CO were approximately 0.13, 0.10, and 0.12, respectively. The Mn_2O_3/SiO_2 sorbent reacted at 0 vol% CO showed the best dechlorination performance. However, there was no significant influence of CO concentration observed on the reaction. Though the SU seemed at first glance to be far lower than expectation, these results could still be considered fairly good in comparison with the capacity of CuO/SiO_2 and Fe_2O_3/SiO_2 sorbents tested in advance.

Fig. 1(b) presents the breakthrough curves for the removal of HCl at various CO concentrations as the concentration of H_2 was changed to 10 vol%. The breakthrough dimensionless time at 0, 10, 25 vol% CO were around 0.14, 0.14, and 0.07, respectively. At 0 and 10 vol% CO, the difference between their SUs was not clear; while at 25 vol% CO, its SU fairly dropped. However, this observation was not in concord with the above results in Fig. 1(a); that is, no conclusion so far can be drawn from the above findings.

As tabulated in Fig. 1(c), the inlet H_2 concentration was 0 vol%. The breakthrough dimensionless time at 0, 10, 25 vol% CO were approximately 0.004, 0.010, and 0.011, respectively. It is notable that an abrupt breakthrough was discovered regardless of the CO concentrations when there was no inlet H_2. The capacity of the Mn_2O_3/SiO_2 sorbent was drastically diminished to a level as if the dechlorination did not happen at all. Unquestionably, H_2 should be considered essential for dechlorination.

It was concluded that H_2 was a key parameter in achieving dechlorination, though its specific cause still remained unknown. The presence of CO may not be sufficient for the dechlorination reaction to take place. Furthermore, the concentration of CO seemed to have no obvious influence on the HCl removal. It was likely that in the presence of H_2, the positive influence of H_2 overpowered that of CO on the absorption reaction. In this case, no matter what the CO concentration was, the benefit it provided was not as significant as that from H_2. However, when there was no H_2 present in the reaction system, the influence of CO started to take over. Though the absence of H_2 led to the great decrease of sorbent capacity, the slightly increasing sorbent performance in Fig. 1(c) with increasing CO concentration may indicate certain positive effect from CO on the absorption.

It was surprising that the above observations were quite

different from the previous literatures (Ko *et al.*, 2004; Ko *et al.*, 2007) where contrary effects of H_2 and CO on the desulfurization were found. The increasing concentration of H_2 reduced the SU of desulfurization while that of CO promoted it, and this phenomenon was related to the water-gas shift reaction (Ko *et al.*, 2004; Ko *et al.*, 2007). It was concluded that in this research chance of the participation of water-gas shift reaction in the dechlorination could be low, since the concentrations of H_2 and CO showed different influence on the HCl removal. Furthermore, the fact that the involvement of H_2 was indispensable for dechlorination but it also decreased the SU of desulfurization may result in certain challenges in achieving the best removal performance for both dechlorination and desulfurization.

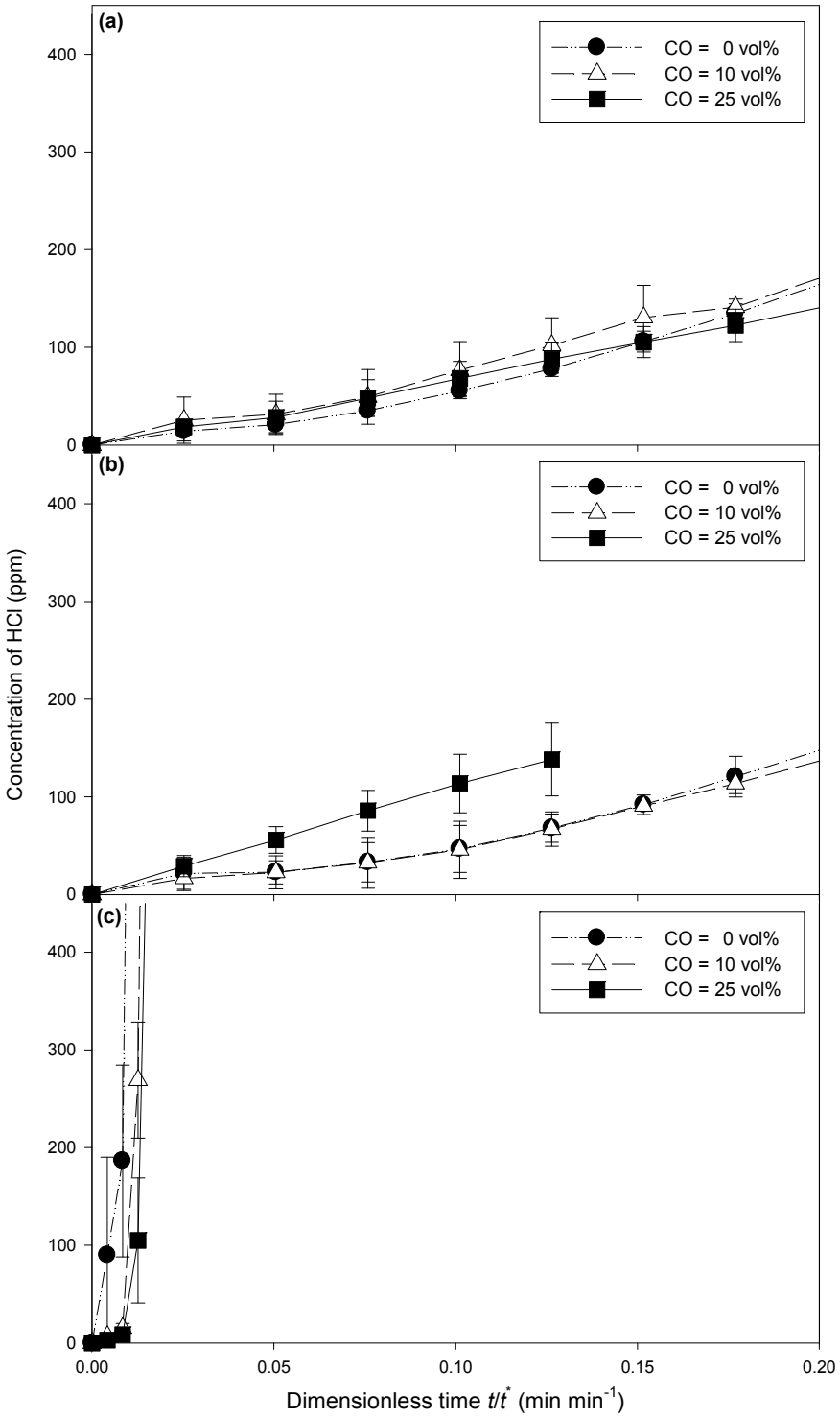

Fig. 1. Breakthrough curves for HCl removal using the Mn_2O_3/SiO_2 sorbent at various CO and H_2 concentrations (673 K, inlet HCl = 3,000 ppm, WHSV = 6,000 mL/h/g) ((a) H_2 = 15 vol%, (b) H_2 = 10 vol%, and (c) H_2 = 0 vol%).

To further confirm the strong influence of the absence of H_2 on the reaction, XRD characterization of the fresh and chlorinated sorbents was carried out. Fig. 2 gives the XRD patterns for eleven samples: one pure SiO_2, one fresh Mn_2O_3/SiO_2 sorbent, and nine sets of chlorinated sorbents. The first XRD patterns were from the pure SiO_2 sorbent. According to the PDF database published by ICDD, the patterns displayed a clear view of SiO_2 (42–1401) in favor of the identification of SiO_2 contained in the following patterns. The second XRD result belonging to the fresh sorbent confirmed that the sorbent initially contained mainly Mn_2O_3 (65–7467) supported by SiO_2. The rest of the XRD patterns were obtained from the previous experiments (Fig. 1). As presented in Fig. 2, after the dechlorination reaction with 3,000 ppm HCl at 0 vol% H_2 and various CO concentrations the three patterns of the chlorinated samples stayed unchanged; that is, due to the absence of H_2 the dechlorination failed to take place. This result was in conformity with previous observations in Fig. 1(c). In addition, patterns assessed from experiments with the involvement of H_2 displayed the transition from the fresh sorbent (Mn_2O_3) to the reacted sorbent (Mn_3O_4, 24–0734). It is worth mentioning that typically in a high-temperature dechlorination process using Mn-based sorbents, the end product was expected to be $MnCl_2$ which was undetected in this XRD patterns. In-depth discussion regarding the

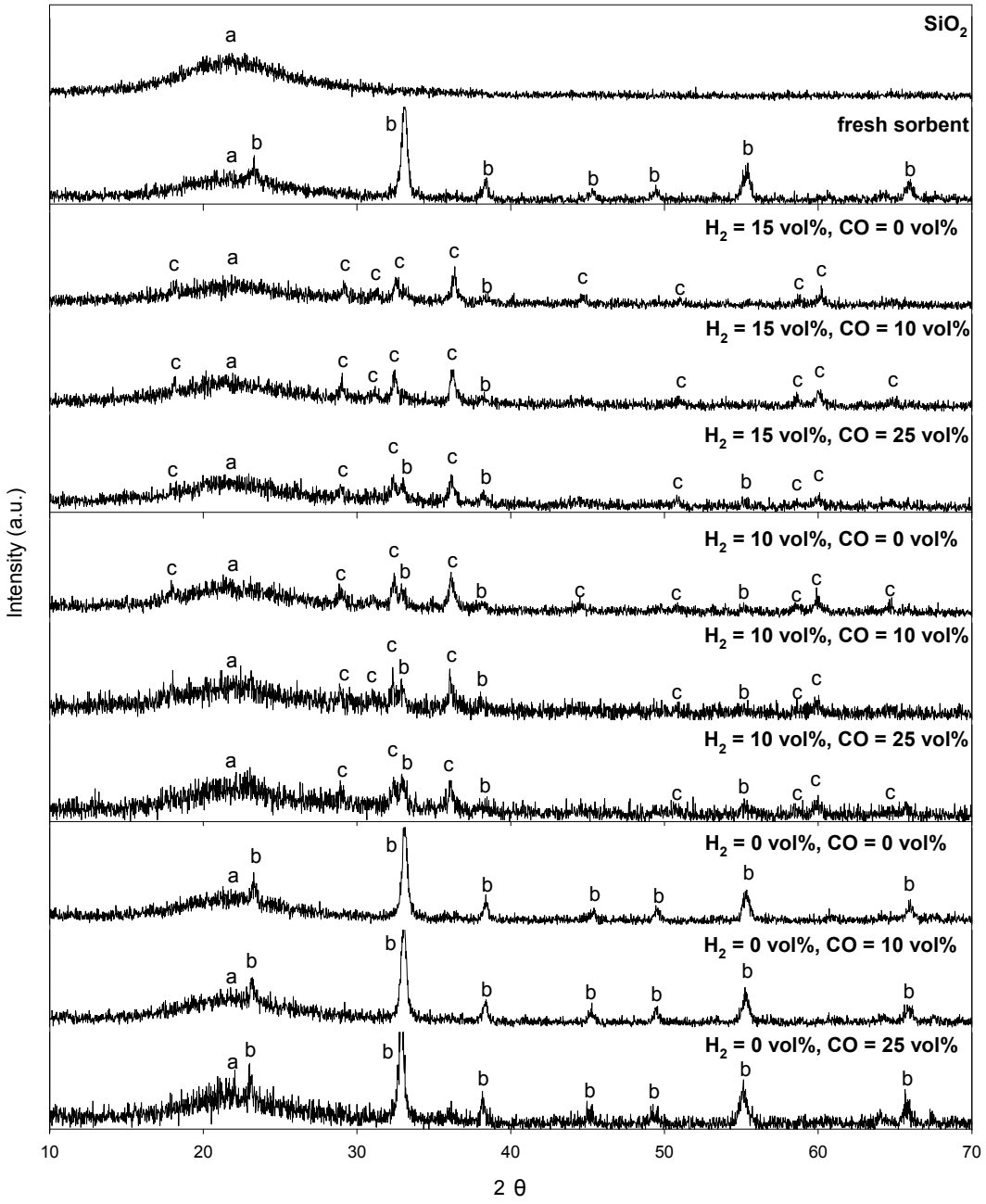

Fig. 2. XRD patterns of the pure SiO_2, fresh sorbent, and chlorinated sorbents at various CO and H_2 concentrations (673 K, inlet HCl = 3,000 ppm, WHSV = 6,000 mL/h/g) ((a) SiO_2, (b) Mn_2O_3, and (c) Mn_3O_4).

confirmation of the presence of $MnCl_2$ in the chlorinated sorbents through X-ray photoelectron spectroscopy (XPS) analysis can be found in our previous investigation where the binding energy of Mn 2p3/2 located at 640.6 eV was assigned to Mn^{2+} in $MnCl_2$ and that of Cl 2p centered around 198.0–199.0 eV corresponded to Cl^- in $MnCl_2$.

Fig. 3 displays the FTIR spectroscopy obtained from the previous HCl removal experiments (Fig. 1). Due to the high concentration of the inlet CO (at 2,030–2,250 cm^{-1}), the spectroscopy was magnified in favor of the observation of other species. In Fig. 3(a) the experiment was implemented with 10 vol% CO and 10 vol% H_2, and the existence of CO_2 (at 2,230–2,450 and 3,500–3,800 cm^{-1}) and H_2O (at 1,300–2,000 and 3,500–4,000 cm^{-1}) confirmed the accuracy of the previous prediction of Reactions (3)–(5). The decreasing absorbance of CO_2 and H_2O was assumed to be related to the exhaustion of Mn_2O_3 contained in the sorbent and the subsequent exhaustion of Mn_3O_4 reduced from Mn_2O_3. Besides, at around 0.15 t/t^* the spectrum patterns of HCl (at 2,700–3,100 cm^{-1}) was observed, in which case it could be concluded that the breakthrough of HCl took place approximately within a dimensionless time range of 0.10–0.15 which was in accordance with the experimental results in Fig. 1(b). Also, the increasing HCl absorbance indicated that the breakthrough of HCl was gradually achieved as the experiment proceeded.

In Fig. 3(b), the FTIR spectroscopy was obtained from the previous dechlorination experiments conducted with 0 vol% CO and 10 vol% H_2 (Fig. 1(b)). The species detected were HCl and H_2O (H_2 cannot be detected by FTIR), which was in concord with the reaction products in Reactions (3)–(5). There was no inlet CO, therefore no CO_2 absorbance was observed. Clearer absorbance peaks of H_2O were found, and its progressively decreasing spectrum pattern was probably due to the exhaustion of Mn_2O_3 and that of Mn_3O_4 reduced from Mn_2O_3 as well. Moreover, the absorbance peak of HCl at 0.15 t/t^* revealed that the breakthrough of HCl also took place approximately within a dimensionless time range of 0.10–0.15, in agreement with the previous experimental data displayed in Fig. 1(b).

As discussed previously, the presence of H_2 had a great effect on the dechlorination reaction. The participation of H_2 was extremely essential for the HCl removal experiments. Fig. 3(c) shows the FTIR spectrum of the outlet gases in the experiment carried out with 10 vol% CO and 0 vol% H_2. The absorbance peaks of H_2O and CO_2 responded to the reaction products in Reactions (3)–(5). The decreasing absorbance of CO_2 and H_2O as the experiment proceeded were resulted from the exhaustion of Mn_2O_3 and Mn_3O_4. Additionally, a large amount of HCl was detected at 0.02 t/t^*, implying that the breakthrough of HCl was achieved at about 0.01–0.02 t/t^* in conformity with previous experimental results in Fig. 1(c).

Reaction Mechanism

Taking above experimental results into consideration, the overall performance of the Mn_2O_3/SiO_2 sorbent seemed inadequate for a complete removal of HCl. However, research into the reaction mechanism behind this complex system can still be beneficial for the future development of dechlorination technology. In order to further explore the reaction chemistry of the Mn_2O_3/SiO_2 sorbent in a chlorine-containing coal gas system, additional information on the XRD patterns for sorbents that had went through experiments without the presence of inlet HCl at various CO and H_2 concentrations was provided in Fig. 4. Different from the previous results, Fig. 4 displays clear patterns of MnO (65–0641), and the remaining Mn_2O_3 contained in the Mn_2O_3/SiO_2 sorbent along with some Mn_3O_4. Interesting inferences can be drawn from the above observations.

Firstly, due to the strong XRD patterns of MnO, it can be assumed that the end product of the experiment carried out without the presence of HCl was MnO. It is obvious that Mn_2O_3 contained in the fresh sorbent (Fig. 2) was reduced into MnO after reacting with CO and/or H_2

Secondly, given the observed Mn_3O_4 patterns in the XRD results (Fig. 4), it can be concluded that the reduction of Mn_2O_3 into MnO was inevitably accompanied by the participation of Mn_3O_4 as a intermediate product.

Thirdly, the existence of HCl was assumed to be able to inhibit Mn_3O_4 from being further reduced into MnO. The Mn_3O_4 would be attacked by HCl to form $MnCl_2$. In addition, in previous XRD results assessed from the chlorinated sorbent (Fig. 2) strong patterns of Mn_3O_4 was detected rather than that of MnO. Combining the above findings, the participation of HCl was able to react with Mn_3O_4 (reduced from Mn_2O_3) to form $MnCl_2$, leading to the failure of the production of MnO. The patterns of Mn_3O_4 in Fig. 2 indicated that in the research conducted with HCl, parts of the Mn_3O_4 was reacted with HCl to produce $MnCl_2$, and the rest of them remained as Mn_3O_4; that is, the existence of HCl could suppress the formation of MnO from the remaining Mn_3O_4. In other words, Mn_2O_3 contained in the fresh sorbent was supposed to be reduced to Mn_3O_4 and then to MnO under the strong reducing atmosphere provided by CO and/or H_2; however, the existence of HCl restrained this tendency.

Fourthly, in Fig. 4 it was found that the coexistence of CO and H_2 in the reaction was not a necessity for the production of MnO. Either CO or H_2 could be the motivation behind the formation of MnO. The only difference was the extent of the reduction of Mn_2O_3, since in Fig. 4 when the inlet concentration of CO was 25 vol% and that of H_2 was 15 vol% almost no XRD patterns of Mn_2O_3 was observed as if its reduction was achieved more completely.

In conclusion, this study has evaluated the effects of CO and H_2 concentrations on the dechlorination experiments, followed by an investigation into the dechlorination mechanism of the Mn_2O_3/SiO_2 sorbent. The parts of the dechlorination mechanism of Mn_2O_3/SiO_2 sorbent were established and the multiple reactions involved were also identified (Reactions (3)–(5)); the Mn_2O_3/SiO_2 sorbent could either react with HCl in the atmosphere of CO and H_2 to form $MnCl_2$, CO_2, and H_2O, or be reduced to Mn_3O_4 and reacted with HCl in the atmosphere of CO and H_2 to produce $MnCl_2$, CO_2, and H_2O.

In elaborating the reactions between the Mn_2O_3/SiO_2 sorbent and HCl accompanied by CO and H_2, Fig. 5 presents

the reaction mechanism comprising three major routes for the dechlorination: (a) the Mn_2O_3 contained in the sorbent reacted with HCl to form $MnCl_2$, (b) Mn_2O_3 was first reduced into Mn_3O_4 and then made contact with HCl to

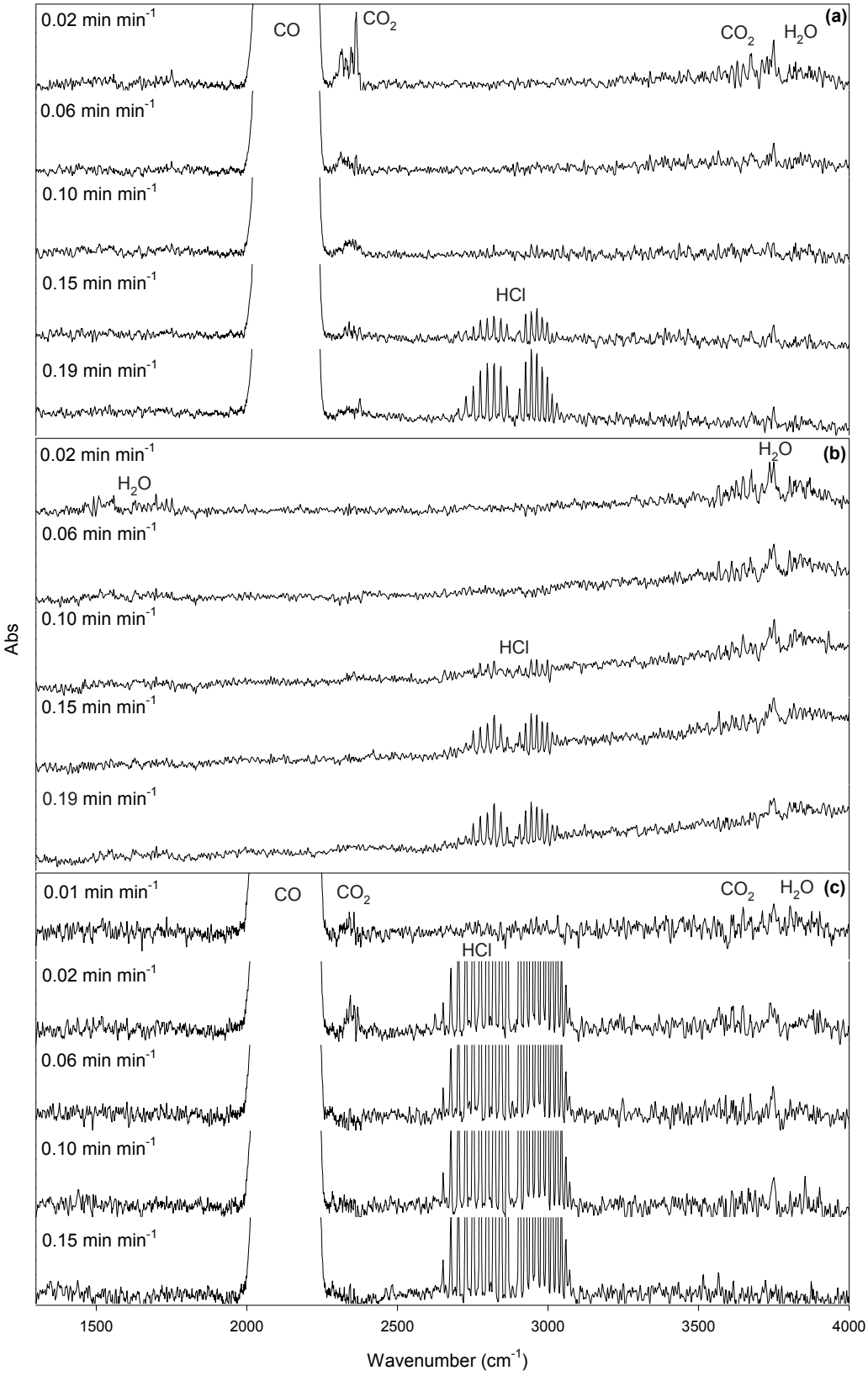

Fig. 3. FTIR spectroscopy for HCl removal using the Mn_2O_3/SiO_2 sorbent (673 K, inlet HCl = 3,000 ppm, WHSV = 6,000 mL/h/g) ((a) CO = 10 vol%, H_2 = 10 vol%, (b) CO = 0 vol%, H_2 = 10 vol%, and (c) CO = 10 vol%, H_2 = 0 vol%).

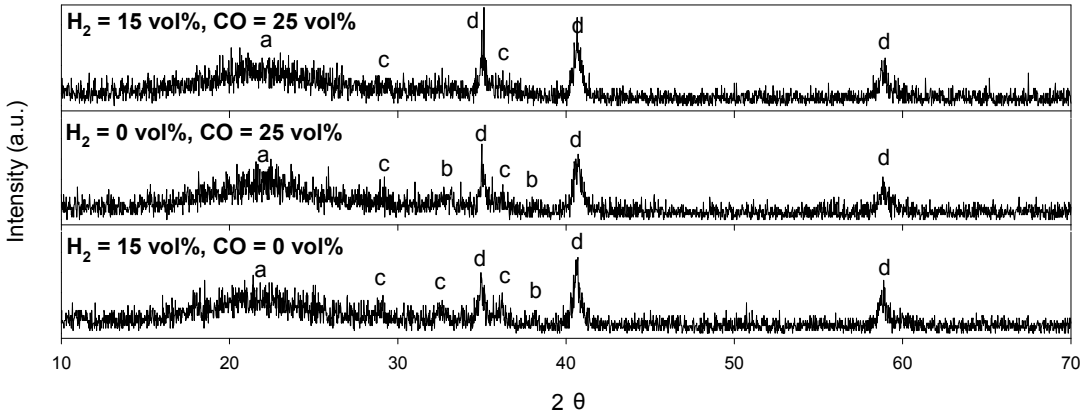

Fig. 4. XRD patterns of chlorinated sorbents at various CO and H_2 concentrations (673 K, inlet HCl = 0 ppm, WHSV = 6,000 mL/h/g) ((a) SiO_2, (b) Mn_2O_3, (c) Mn_3O_4, and (d) MnO).

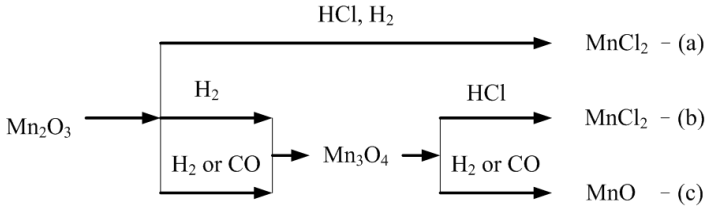

Fig. 5. Reaction mechanism for HCl removal using the Mn_2O_3/SiO_2 sorbent (673 K, WHSV = 6,000 mL/h/g).

produce $MnCl_2$, and (c) in the absence of inlet HCl, Mn_2O_3 was firstly reduced to Mn_3O_4 and then to MnO (Fig. 4). As can be seen from Fig. 5, in route (a), H_2 was found to be essential for the dechlorination (Fig. 1(c)); that is, for the production of $MnCl_2$ the involvement of HCl and H_2 was critical, and that of CO was relatively insignificant. In route (b), the fact that without the presence of H_2 the Mn_2O_3 sorbent showed almost no reactivity with inlet HCl after the dechlorination (Fig. 2) implied the formation of Mn_3O_4 and $MnCl_2$ required the participation of H_2. In route (c), the three well-detected patterns of MnO in Fig. 4 inferred the coexistence of CO and H_2 in the simulated gas was not indispensable for the reduction of Mn_2O_3 into Mn_3O_4 and MnO. Either the presence of CO or H_2 could benefit the formation of MnO.

CONCLUSIONS

This study aims at the evaluating the influence of CO and H_2 concentrations on the performance of HCl elimination. The experiments were conducted in a fixed-bed reactor at 673 K by supported manganese oxide sorbent, Mn_2O_3/SiO_2, at various CO and H_2 concentrations. The absence of inlet H_2 led to a drastic diminishment of the sorbent capacity. It was concluded that the participation of H_2 was an indispensable requirement in achieving dechlorination by the Mn_2O_3/SiO_2 sorbent though its specific cause still remained unknown. Furthermore, the concentration of CO seemed to have no obvious influence on the HCl removal.

Through the breakthrough experiments, XRD and FTIR analysis, this study also reports on a deeper investigation into the chemistry of the Mn_2O_3/SiO_2 sorbent in a chlorine-containing coal gas system. Three major routes in the dechlorination mechanism comprising the formation of $MnCl_2$ from the reaction of Mn_2O_3 or Mn_3O_4 with HCl, the reduction of Mn_2O_3 into Mn_3O_4, and the production of MnO were successfully established.

It is worth mentioning that the SU in this study seemed to be far lower than expectation, due to the unknown reactions taking place in this complex chlorine-containing coal gas system. It was concluded that the reactivity between the Mn_2O_3/SiO_2 sorbent and the inlet simulated gas environment containing HCl, CO, and H_2 was not as good as expected. In this research the laboratory scale experiment indicated that the dechlorination performance of Mn_2O_3/SiO_2 sorbent was not good. Though the dechlorination mechanism of the Mn_2O_3/SiO_2 sorbent was successfully built in this study, the reason behind its low capacity still suggested the necessity for further study.

REFERENCES

Atimtay, A.T. (2001). Cleaner Energy Production with Integrated Gasification Combined Cycle Systems and Use of Metal Oxide Sorbents for H_2S Cleanup from Coal Gas. *Clean Technol. Environ. Policy* 2: 197–208.

Bakker, W.J.W., Kapteijn, F. and Moulijn, J.A. (2003). A High Capacity Manganese-Based Sorbent for Regenerative High Temperature Desulfurization with Direct Sulfur Production Conceptual Process Application to Coal Gas Cleaning. *Chem. Eng. J.* 96: 223–235.

Bu, X.P., Ying, Y.J., Zhang, C.Q. and Peng, W.W. (2008). Research Improvement in Zn-Based Sorbent for Hot Gas Desulfurization. *Powder Technol.* 180: 253–258.

Chang, C.P., Shen, Y.H., Chou, I. C., Wang, Y.F., Kuo, Y.M. and Chang, J.E. (2012). Metal Distribution Characteristics in a Laboratory Waste Incinerator. *Aerosol Air Qual. Res*. 12: 426–434.

Chin, T., Yan, R. and Liang, D.T. (2005). Study of the Reaction of Lime with HCl under Simulated Flue Gas Conditions Using X-ray Diffraction Characterization and Thermodynamic Prediction. *Ind. Eng. Chem. Res*. 44: 8730–8738.

Dean, J.A. (1979). *Lange's Handbook of Chemistry*, 12th Edition, McGraw-Hill, New York, p. 9-4–9-94.

Dou, B.L., Chen, B.B., Gao, J.S. and Sha, X.Z. (2005). Reaction of Solid Sorbents with Hydrogen Chloride Gas at High Temperature in a Fixed-Bed Reactor. *Energy Fuels* 19: 2229–2234.

Kiil, S., Nygaard, H. and Johnsson, J.E. (2002). Simulation Studies of the Influence of HCl Absorption on the Performance of a Wet Flue Gas Desulphurisation Pilot Plant. *Chem. Eng. Sci.* 57: 347–354.

Ko, T.H., Chu, H., Chaung, L.K. and Tseng, T.K. (2004). High Temperature Removal of Hydrogen Sulfide Using an N-150 Sorbent. *J. Hazard. Mater.* 114: 145–152.

Ko, T.H., Chu, H. and Chaung, L.K. (2005). The Sorption of Hydrogen Sulfide from Hot Syngas by Metal Oxides over Supports. *Chemosphere* 58: 467–474.

Ko, T.H., Chu, H. and Tseng, J.J. (2006). Feasibility Study on High-Temperature Sorption of Hydrogen Sulfide by Natural Soils. *Chemosphere* 64: 881–891.

Ko, T.H., Chu, H., Lin, H.P. and Peng, C.Y. (2006). Red Soil as a Regenerable Sorbent for High Temperature Removal of Hydrogen Sulfide from Coal Gas. *J. Hazard. Mater.* 136: 776–783.

Ko, T.H., Chu, H. and Liou, Y.J. (2007). A Study of Zn-Mn Based Sorbent for the High-Temperature Removal of H_2S from Coal-Derived Gas. *J. Hazard. Mater.* 147: 334–341.

Krishnan, G.N., Wood, B.J., Canizales, A., Gupta, R., Sheluker, S.D. and Ayala, R. (1994). Development of Disposal Sorbents for Chloride Removal from High-Temperature Coal-Derived Gases, Coal-fired Power Systems 94 Advances in IGCC and PFBC Review Meeting, U.S. Department of Energy, Office of Fossil Energy, Morgantown Energy Technology Center, West Virginia, June 21–23.

Li, Y.R., Qi, H.Y., You, C.F. and Xu, X.C. (2007). Kinetic Model of CaO/Fly Ash Sorbent for Flue Gas Desulphurization at Moderate Temperatures. *Fuel* 86: 785–792.

Lin, W.Y., Wu, Y.L., Tu, L.K., Wang, L.C. and Lu, X. (2010). The Emission and Distribution of PCDD/Fs in Municipal Solid Waste Incinerators and Coal-Fired Power Plant. *Aerosol Air Qual. Res*. 10: 519–532.

Lou, J.C., Yang, H.W. and Lin, C.H. (2009). Preparing Copper/Manganese Catalyst by Sol–Gel Process for Catalytic Incineration of VOCs. *Aerosol Air Qual. Res*. 9: 435–440.

Nunokawa, M., Kobayashi, M. and Shirai, H. (2008). Halide Compound Removal from Hot Coal-Derived Gas with Reusable Sodium-Based Sorbent. *Powder Technol.* 180: 216–221.

Tseng, T.K., Chang, H.C., Chu, H. and Chen, H.T. (2008). Hydrogen Sulfide Removal from Coal Gas by the Metal-Ferrite Sorbents Made from the Heavy Metal Wastewater Sludge. *J. Hazard. Mater.* 160: 482–488.

Tu, L.K., Wu, Y.L., Wang, L.C. and Chang-Chien, G.P. (2011). Distribution of Polybrominated Dibenzo-*p*-dioxins and Dibenzofurans and Polybrominated Diphenyl Ethers in a Coal-fired Power Plant and Two Municipal Solid Waste Incinerators. *Aerosol Air Qual. Res*. 11: 596–615.

Wakker, J.P., Gerritsen, A.W. and Moulijn, J.A. (1993). High Temperature H_2S and COS Removal with MnO and FeO on γ-Al_2O_3 Acceptors. *Ind. Eng. Chem. Res.* 32: 139–149.

Westmoreland, P.R. and Harrison, D.P. (1976). Evaluation of Candidate Solids for High-Temperature Desulfurization of Low-Btu Gases. *Environ. Sci. Technol.* 10: 659–661.

Yan, R., Chin, T., Liang, D.T., Laursen, K., Ong, W.Y., Yao, K. and Tay, J.H. (2003). Kinetic Study of Hydrated Lime Reaction with HCl. *Environ. Sci. Technol.* 37: 2556–2562.

Yang, D., Chen, G. and Zhang, R. (2006). Estimated Public Health Exposure to H_2S Emissions from a Sour Gas well Blowout in Kaixian County, China. *Aerosol Air Qual. Res*. 6: 430–443.

Received for review, February 14, 2012
Accepted, July 19, 2012